SynBio

MDPI

Article

Streamlined Production, Protection, and Purification of Enzyme Biocatalysts Using Virus-like Particles and a Cell-Free Protein Synthesis System

Seung O. Yang, Joseph P. Talley, Gregory H. Nielsen, Kristen M. Wilding and Bradley C. Bundy *

Department of Chemical Engineering, Brigham Young University, Provo, UT 84602, USA
* Correspondence: bundy@byu.edu

Abstract: Enzymes play an essential role in many different industries; however, their operating conditions are limited due to the loss of enzyme activity in the presence of proteases and at temperatures significantly above physiological conditions. One way to improve the stability of these enzymes against high temperatures and proteases is to encapsulate them in protective shells or virus-like particles. This work presents a streamlined, three-step, cell-free protein synthesis (CFPS) procedure that enables rapid in vitro enzyme production, targeted encapsulation in protective virus-like particles (VLPs), and facile purification using a 6× His-tag fused to the VLP coat protein. This process is performed in under 12 h and overcomes several limitations of enzyme encapsulation, such as the control of packing density, speed, and complexity of the process. Here, we encapsulate the enzyme *Candida antarctica* lipase B in the VLP from the bacteriophage Qβ, while in the presence of a linking RNA aptamer. The encapsulated enzymes largely retained their activity in comparison to the free enzymes. Additionally, when subjected to 90 °C temperatures or 5 h incubation with proteases, the encapsulated enzymes maintained their activity, whereas the free enzymes lost their activity. In this work, we also demonstrate control over packing density by achieving packing densities of 4.7 and 6.5 enzymes per VLP based off the concentration of enzyme added to the encapsulation step.

Keywords: cell-free protein synthesis; virus-like particle; Qβ VLP; CalB; *Candida antarctica* lipase B; enzyme stabilization

Academic Editor: Naglis Malys

Received: 21 December 2024
Revised: 17 January 2025
Accepted: 24 January 2025
Published: 5 February 2025

Citation: Yang, S.O.; Talley, J.P.; Nielsen, G.H.; Wilding, K.M.; Bundy, B.C. Streamlined Production, Protection, and Purification of Enzyme Biocatalysts Using Virus-like Particles and a Cell-Free Protein Synthesis System. *SynBio* **2025**, *3*, 5. https://doi.org/10.3390/synbio3010005

1. Introduction

Enzymes catalyze a wide variety of biochemical reactions and are used in many industries including the dairy, textile, food processing, detergent, biofuel, medical diagnostic, therapeutic, paper, and chemical processing industries [1–6]. Advantages of these enzyme biocatalysts include efficiency, rapid kinetics, specificity, and biodegradability. However, instability against small changes in temperature, pH, ionic strength, and solvent hydrophilicity constrain the application of these biocatalysts to more physiological conditions [7–9]. While many technologies for enzyme immobilization have been developed to overcome these limitations—such as adsorption, covalent bonding, entrapment, and cross-linking, these technologies often create new challenges such as limiting the diffusion of reactants and products. Enzyme stabilization by encapsulation inside virus protein capsid shells is a particularly attractive technology as the diffusion of reactants and products can readily occur through natural pores [7,10–26]. Enzyme encapsulation inside these virus-like particles (VLPs) has demonstrated promise in a variety of fields, including drug delivery, enzyme stabilization, and improved chemical synthesis [7,27–29]. Current approaches to

the preparation of VLP-encapsulated enzymes often rely on the in vivo co-production of the VLP and the cargo protein, which limits control of packing density and restricts protein cargo to proteins which can be expressed well under conditions similar to the VLP [30–32]. Here, we present a simple, three-step protein synthesis technology to rapidly produce and selectively encapsulate desired enzymes into protective VLPs, followed by their subsequent purification. This work enables the modification of packing density and differing synthesis conditions for the VLP and cargo.

Viruses have evolved for millions of years to encapsulate and protect specific guest molecules such as nucleic acids and enzymes from biologically unfriendly environments [26]. Inspired by biomimicry, nanotechnologists have engineered the production of protective protein shells or VLPs and have demonstrated selective encapsulation [33,34]. VLP from the bacteriophage Qβ is an excellent candidate for such an application because (1) the Qβ VLP is stabilized by 180 disulfide bonds which helps protect it against higher [34] temperatures (up to 100 °C) and acidic/basic conditions (pH from 3 to 10) [35,36], (2) the Qβ VLP possesses binding specificity towards the RNA of the bacteriophage, which can be exploited for selective encapsulation of enzymes [37,38], (3) the pores at the Qβ VLP's five- and six-fold axis of symmetry allow small molecules—such as substrates and products—to penetrate through the capsid, while preventing the entry of macromolecules such as proteases [39,40], (4) the Qβ VLP is assembled from 180 copies of the same coat protein and the expression of just the coat protein enables its assembly [40], and (5) the Qβ coat protein that assembles into a VLP is readily expressed in *E. coli*, an inexpensive host, or in cell-free proteins synthesis (CFPS) made with *E. coli* extract (minimizing costs is critical for lower margin applications of catalysis) [36,39].

Inspired by the recent successful demonstration of significant enzyme stabilization following encapsulation in the Qβ VLP with in vivo *E. coli* expression, here we engineer this capability into cell-free protein synthesis. Cell-free protein synthesis has a number of advantages, including (1) rapid protein production in a few hours, (2) on demand production for quick response to market demands, (3) direct access to facilitate dynamic optimization and the production of complex proteins, (4) scalability reliably demonstrated from the microliter to the 100+ liter scale, and (5) automation compatibility for labor-free manufacturing [41–45].

Using cell-free protein synthesis (CFPS), we demonstrate the production of *Candida antarctica* lipase B (CalB) as a model enzyme, protect CalB by encapsulation inside Qβ VLP produced in a second CFPS reaction, and purify the CalB-encapsulated VLP, all in less than 12 h (Figure 1). CalB is a widely used lipase, especially in organic polymer synthesis, due to its regio-/enantio-selectivity, stability, compatibility with organic solvents, and wide variety of substrate selectivity [46–50]. CalB belongs to the α/β-hydrolase family and possesses a catalytic triad that consists of Ser-His-Asp [51,52]. There are 317 amino acids in the polypeptide chain with a total molecular mass of about 33 kDa. Three disulfide bridges stabilize the conformation [49].

In addition to the production of purified and encapsulated CalB, we demonstrate controlled enzyme encapsulation efficiency by adding a varying amount of CalB to the CFPS reaction that produces the Qβ VLP. This demonstrates that CFPS can be useful in overcoming the limitation of packing density control that is seen in traditional encapsulation methods. Additionally, an RNA aptamer facilitates the selective VLP encapsulation of the target enzyme. This work also demonstrates that the encapsulated CalB possesses similar kinetic parameters to free CalB, showing that enzymatic activity can be largely conserved upon enzyme encapsulation Most importantly, encapsulated CalB exhibits substantially improved stability against temperatures elevated beyond the melting point of

CalB and encapsulated CalB was resistant against proteases which completely eliminated free CalB activity.

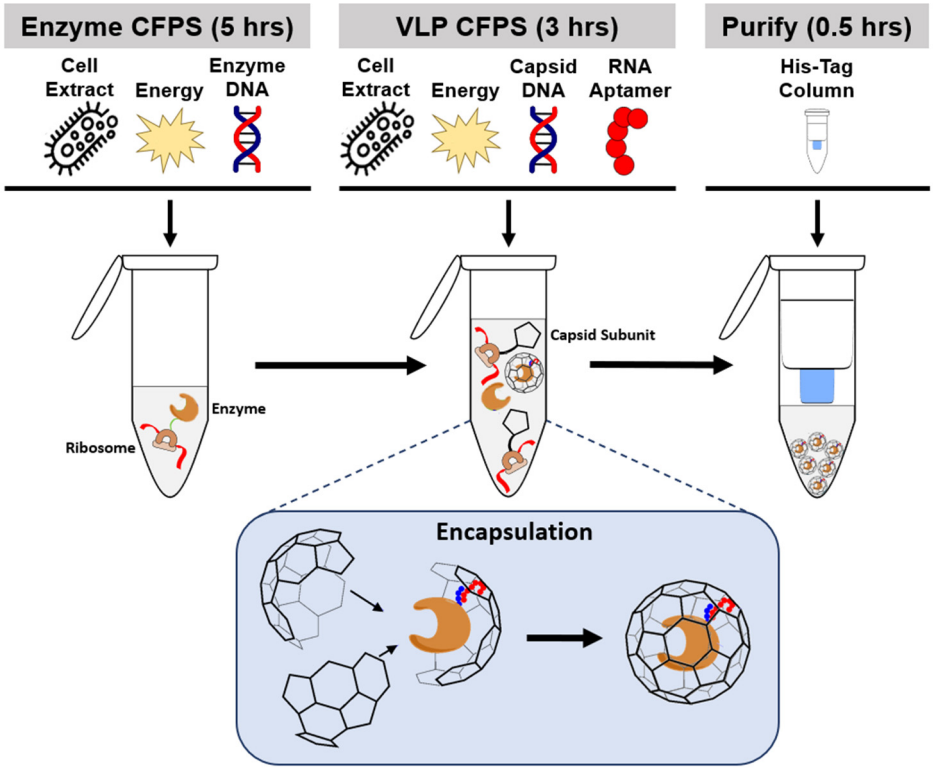

Figure 1. Illustration of the encapsulation process of the enzyme CalB by the bacteriophage Qβ using cell-free protein synthesis and spin column purification. This is a three-step process where CalB is synthesized in an initial cell-free reaction with a Rev tag. The Qβ monomers are synthesized in a second cell-free reaction with a His tag. Encapsulation occurs by directly adding the synthesized CalB from the first reaction into the second. Additionally, an RNA aptamer which binds to the Rev tag on CalB and also to the interior of the Qβ VLP, was added to the second reaction to facilitate CalB encapsulation. Finally, the encapsulated enzymes are recovered using a HisPur^{TM} Ni-NTA spin column.

2. Results

In this work, we produce and encapsulate the lipase CalB into VLPs using CFPS and the bacteriophage Qβ coat protein. This process along with the purification of the encapsulated enzyme can be accomplished in under 12 h using three simple steps, as illustrated in Figure 1.

2.1. CFPS Expression of CalB Enzyme

To improve the soluble yield of the recombinant lipase in our cell-free system, an *E. coli* strain that has overexpressed GroEL and GroES chaperones was prepared as described in prior work [47]. Glutathione buffer (5 mM) was added to the CalB CFPS reaction at a fixed ratio of 4 glutathione oxidized (GSSG) to 1 reduced (GSH) at 30 °C. Using this CFPS reaction, 67 ± 7% of the recombinant CalB lipase produced was soluble and the mean soluble yield was 341 ± 30 ng/µL.

2.2. Targeted Rev-CalB Encapsulation Using Qβ VLP

To facilitate RNA aptamer-guided enzyme encapsulation, an arginine-rich peptide (Rev) tag was fused to the N-terminus of CalB. The completed, unpurified Rev-CalB-producing CFPS reaction was directly transferred to a second CFPS reaction producing

Qβ coat protein (step 2). The mean concentration of soluble Qβ coat protein produced when in the presence of Rev-CalB and the RNA aptamer was 294 ± 24 ng/μL in 160 μL CFPS reaction.

To facilitate enzyme encapsulation, 10 μg of RNA aptamer (containing the Rev tag binding RNA sequence linked to the Qβ hairpin loop sequence that natively binds to the inner surface of the Qβ VLP) was added to the VLP-synthesizing CFPS reaction (step 2). The autoradiogram analysis reported the necessity of the RNA aptamer for the significant encapsulation of Rev-CalB (Figures 2a and S2). The VLP synthesized by CFPS with the RNA aptamer sample contained a Rev-CalB protein band while the VLP synthesized by CFPS without the aptamer showed no Rev-CalB protein band (Figure 2a). This result is consistent with additional experiments encapsulating superfolder green fluorescent protein (sfGFP) in place of CalB (Figure S1). To further test for the random encapsulation of non-target proteins during the VLP assembly, Qβ coat protein was expressed by CFPS using a cell lysate that contained sfGFP. Assembled VLPs were purified via a size-exclusion column, and sfGFP activity was not detected in purified VLPs but only detected in the flow through samples with other proteins that were not encapsulated in the VLP (Figure S1). This observation is consistent with the data in Figure 2a, where CalB encapsulation was detected when the RNA aptamer was added to the VLP-producing and assembling reaction and a discernable band was not observed when the aptamer was not added.

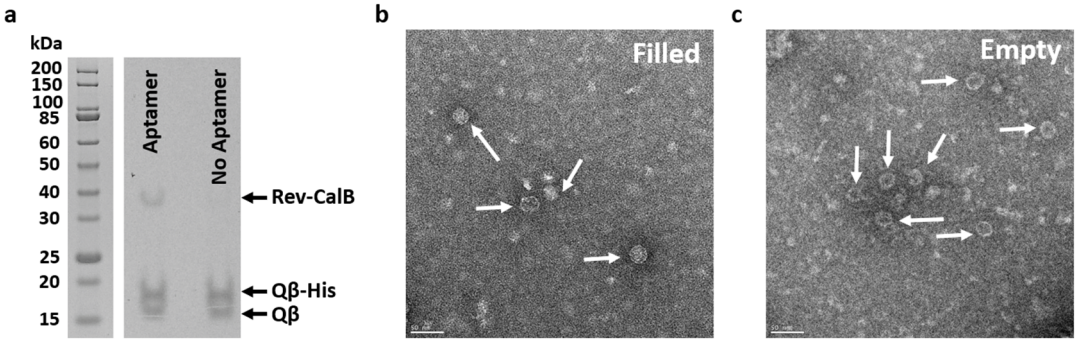

Figure 2. (**a**) Autoradiogram analysis of Qβ VLPs from CFPS reactions in the presence of Rev-CalB with and without added RNA aptamer. The absence of a Rev-CalB band when RNA aptamer was not added shows that encapsulation is ineffective without the aptamer. The protein molecular weight ladder (**left**) is from the original SDS-PAGE gel used to develop the autoradiogram (**right**) and is aligned to the developed autoradiogram. (**b**,**c**) TEM images of filled and unfilled VLPs. The arrows indicate locations of VLPs. The white scale bar in the bottom left corner of each image represents a size of 50 nm.

Transmission electron microscopy (TEM) was used to confirm whether the VLPs were filled or empty, as well as to verify their respective sizes (Figure 2b,c). The samples were negatively stained with 0.2% phosphotungstic acid [39]. Filled VLPs appear more stained on TEM images than empty ones. The free and encapsulated mean VLP diameters were 25.0 ± 1.8 and 26.3 ± 2.8 nm, respectively, which is similar to the previously reported diameter of the Qβ VLP (~25–28 nm) [40].

The enzyme encapsulation efficiency was tested by adding various amounts of Rev-CalB to the VLP synthesizing CFPS reaction (step 2) while holding the amount of RNA aptamer fixed. The densitometry analysis of the VLP showed that the increased Rev-CalB in the VLP synthesis reaction correlated with a greater number of encapsulated enzymes. This correlation suggests an ability to control the VLP encapsulation density by altering the amount of cargo protein added to the reaction. There is a concentration threshold requirement with no detectable encapsulation by densitometry at lower than 53 ng/μL of CalB (8.4 μg or less of enzyme added to a 160 μL reaction). At a concentration of

87 ng/µL of CalB in the CFPS reaction producing VLP (13.9 µg of enzyme added to a 160 µL reaction), an average of 4.7 Rev-CalB enzymes encapsulated per VLP was observed by the densitometry analysis (Figure S3c,d). At a concentration of 106 ng/µL of CalB in the CFPS reaction producing VLP (17 µg of enzyme added to a 160 µL reaction), an average of 6.5 Rev-CalB enzymes encapsulated per VLP was observed (Figure S3b). It should be noted that only 12% of the total added Rev-CalB was encapsulated as the rest was located in the purification flow through. This is likely due to steric hindrance.

2.3. Purification of Qβ-Encapsulated CalB via Spin His-Column

Here, we demonstrate a six-Histidine tag fused onto the Qβ coat protein as an efficient method to purify the VLP using a spin nickel affinity column. The recent extension of endotoxin-free protein synthesis to CFPS could allow similar minimal purification schemes to be sufficient for medically applicable VLP-encapsulated enzymes [53]. The purification process yielded a 70% recovery of the VLPs, as measured by scintillation counting and a densitometry analysis (Figure S3a,b).

2.4. Enzyme Activity

To test the functional capabilities of the encapsulated lipases, activities of both free and encapsulated enzymes were compared using the chromogenic substrate 4-nitrophenyl octanoate (Figure 3) [54]. For this comparison VLP encapsulated with an average of 4.7 Rev-CalB per capsid was used (13.9 µg of Rev-CalB was added to a 160 µL CFPS reaction producing the VLP). The kinetic data from a standard Michaelis–Menten analysis for both the free and encapsulated enzymes were normalized to the same quantity of protein. The data showed that both enzymes possess similar parameters with k_{cat}/K_M values of 3080 ± 210 and 3300 ± 850 M^{-1} s^{-1} for the free and the encapsulated lipases, respectively (Table 1). The difference in enzyme activity between the free and encapsulated lipases was small. The enzyme's turnover numbers were 0.71 ± 0.02 and 0.49 ± 0.04 for the free and the encapsulated forms, respectively. The observed k_{cat} and k_{cat}/K_M values are comparable to those reported for hydrolysis of 4-nitrophenyl ester substrates [54]. Moderately decreased K_M values were observed upon encapsulation as well.

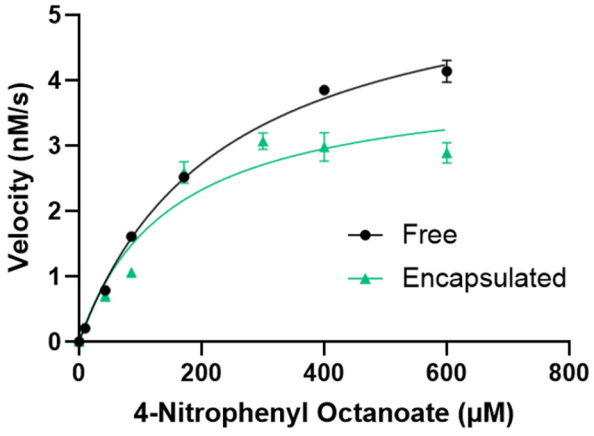

Figure 3. Enzymatic activity of free versus VLP-encapsulated Rev-CalB using the substrate 4-nitrophenyl octanoate. Kinetic data were obtained from standard Michaelis–Menten analysis using GraphPad Prism 10 software. Error bars represent the standard deviation from n = 3 assays.

Table 1. Michaelis–Menten parameters for free versus encapsulated Rev-CalB obtained using GraphPad Prism 10 software. ± values represent the standard deviation from $n = 3$ assays.

	V_{max} (nM/s)	K_{cat} (s^{-1})	K_m (μM)	K_{cat}/K_m (M^{-1} s^{-1})
Free	5.88 ± 0.16	0.71 ± 0.02	232 ± 15	3080 ± 210
Encapsulated	4.05 ± 0.34	0.49 ± 0.04	149 ± 36	3300 ± 850

The specific activities of the encapsulated enzymes produced with 13.9 and 17 μg of added enzyme to the 160 μL encapsulation reaction were calculated and plotted in comparison to the added enzyme quantities (Figure 4). The data indicate that, with higher packaging densities of CalB inside the VLP, there is a slight decrease in the specific activity. This is somewhat expected as the more crowded environment would increase CalB-CalB and CalB-Qβ interactions, which could have a negative effect on enzyme flexibility and activity.

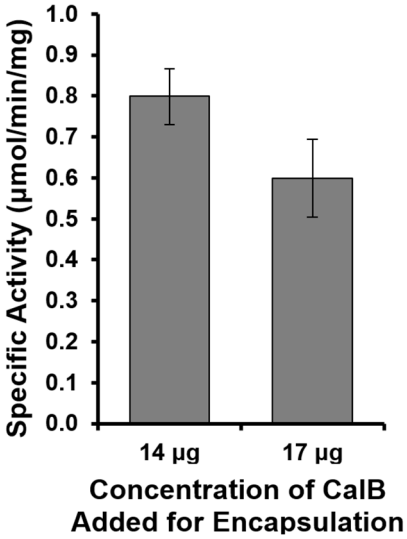

Figure 4. Specific activity of Rev-CalB (μmol/min/mg) encapsulated in VLP, where 14 μg or 17 μg unpurified Rev-CalB from the first CFPS reaction was added to a second 160 μL CFPS reaction wherein the Qβ coat protein was produced and assembled. A moderate drop in specific activity was observed for the VLP sample with a higher number of VLP encapsulated on average. Error bars represent the standard deviation from $n = 3$ assays.

2.5. Enzyme Stability

While there was a moderate drop in the activity of CalB when encapsulated in the VLP (Figure 3), the VLP served to stabilize the encapsulated Rev-CalB, allowing the VLP-encapsulated enzyme to withstand high temperatures. Free and encapsulated enzymes were first incubated at varying temperatures (37, 60, 75, and 90 °C) for 20 min followed by 1 h of incubation at the optimum temperature of 37 °C (Figure 5a) [55]. In this study, encapsulated VLP contained an average of 4.7 Rev-CalB per VLP. The enzyme activity at each temperature was normalized by the activity at the optimum temperature. Almost all the free enzyme activity was lost when incubated at 60 °C or above, while the encapsulated enzymes maintained their activity even at 90 °C. For reference, the reported melting temperature of CalB is 57.7 °C [56].

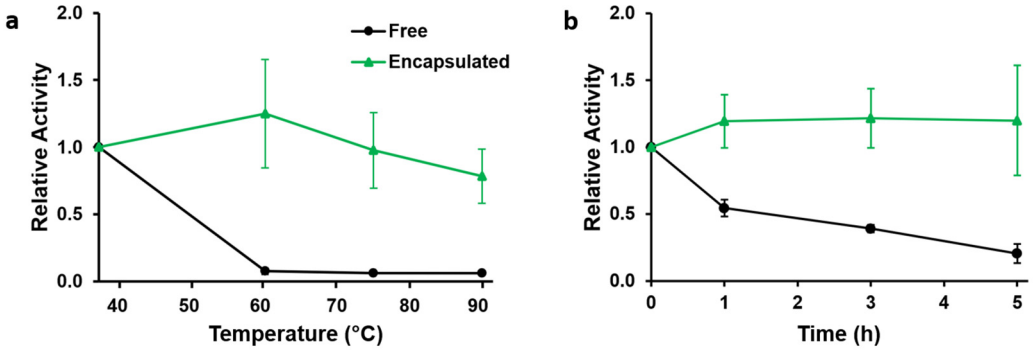

Figure 5. Relative enzymatic activity of free versus encapsulated Rev-CalB under different conditions. (**a**) The plot shows the effect of temperature on enzymatic activity. Enzymes were incubated at different temperatures for 20 min before being incubated at 37 °C for one hour. (**b**) The plot shows the enzymatic activity in the presence of proteinase K over time. Enzymes were incubated at 37 °C in the presence of the protease. Under both conditions, the encapsulated enzyme showed an improved relative activity. Error bars represent data from $n = 3$ measurements.

VLP encapsulation also significantly stabilized the encapsulated enzyme against protease degradation, consistent with previous reports [38]. Free and encapsulated enzymes were incubated at 37 °C with varying incubation times in the presence of proteinase K (Figure 5b) and then directly assessed for activity with the substrate 4-nitrophenyl octanoate. All the enzyme activities were normalized by the activity obtained before initiating incubation with proteinase K. The free enzyme activity dropped by a factor of 2 after 1 h of incubation with the protease and only about 20% of the activity remained after 5 h. However, the encapsulated enzyme maintained its full activity over a 5 h incubation period with the protease. These data indicate that the VLP provides protection and stability to guest molecules.

3. Discussion

This work harnesses the capabilities of cell-free protein synthesis to streamline the process of producing, encapsulating, and purifying biocatalysts for use in a wide variety of fields. Virus-like particles provide these enzymes with stability in a range of conditions. While the traditional production and encapsulation of enzymes suffers from low yields, slow production times, and the inability to manipulate the packing density of the enzymes, CFPS enabled a simple and fast workflow that achieved appreciable yields while also being able to change the packing density (Figure 1).

3.1. CFPS Expression of CalB Enzyme

Many eukaryotic microorganisms have been used for the expression and protein engineering of CalB lipase [49,57–60]. There have been previous attempts to synthesize CalB in *E. coli* periplasm and cytoplasm [46,49,61]. Disadvantages of these methods include the low soluble lipase yield and inclusion body formation, the latter being a result of using temperatures higher than 20 °C in the *E. coli* expression system [62]. At 20 °C, CalB expression takes about two days to get a satisfactory amount of soluble lipase. With cell-free protein synthesis, we report satisfactory yields of soluble lipase upon synthesis which requires a total of 5 h. CFPS is often able to synthesize proteins that form inactive aggregates or inclusion bodies in vivo because (1) the cell-free environment is 20-fold less crowded than that inside a cell, (2) translation rates are slower due to the diluted environment and can further decreased by decreasing the temperature of the CFPS reaction, and (3) folding chaperone concentration can be directly optimized due to the open nature of cell-free systems.

3.2. Targeted Rev-CalB Encapsulation Using Qβ VLP

The open reaction environment of CFPS enabled the control of the encapsulation efficiency of CalB by the Qβ VLP. By adding varying amounts of CalB to the second cell-free reaction, the average number of CalB per VLP was tuned. This is important as a higher packing efficiency did lead to a modest drop in activity, while lower packaging efficiencies require more VLPs and thus the synthesis of more Qβ coat protein per CalB enzyme. The cell-free system enables tuning such parameters toward optimizing CalB activity, stability, and total reagent costs. The theoretical maximum number of CalB enzymes that would fit into the Qβ VLP is approximately 51, based off an inner VLP diameter of 21.4 nm and CalB volume of 60 cubic nm [26,63]. In reality, the number is likely to be much smaller due to the need for the binding of CalB to the inner wall of the VLP for efficient encapsulation as well as steric hindrance. Another area for future optimization is the aptamer size. During the encapsulation process, the number of enzymes enclosed in the VLP is limited by size and the ability of the VLP to properly form. It is possible that the length of the aptamer may play a role in encapsulation efficiency as it is 646 nucleotides long. Shorter aptamers may help to encompass more guest enzymes. Additional testing is needed to determine the effect aptamer length plays and what aptamer length is optimal for the system.

3.3. Purification of Qβ-Encapsulated CalB via Spin His-Column

The conventional way of purifying VLP is by using either sucrose density gradients or size exclusion columns. While both methods are excellent in VLP purification, they are time-consuming, labor-intensive, and sensitive to vibration, jolt, and tilt. In this work, a histidine tag provides a faster and efficient method to purify the VLPs. It is important to note that two different plasmids for the Qβ monomers were used: one with the His tag and one without. The reason for this is that the use of solely His tag monomers prevents the assembly of the capsid, whereas using both types of monomer allows for assembly to occur as well as subsequent purification.

3.4. Enzyme Activity

The activities of both the free and encapsulated enzymes were compared using the substrate 4-nitrophenyl octanoate. The kinetic parameters from the Michaelis–Menten analysis for both enzymes were similar. The K_M value decreased upon encapsulation. One possible explanation is that the addition of the RNA aptamer which allows for the binding of CalB to the inner surface of the VLP causes the interfacial activation of CalB to occur where the lid type structure shielding the active site opens, thereby allowing the substrate to bind better [64]. Another possibility is that encapsulation restricts the movement of the enzyme, increasing positive interactions with the substrate. Additionally, the formation of the VLP may create a microenvironment inside, which increases the substrate binding affinity of CalB. Decreased K_M and enzyme activity upon encapsulation was seen in a previous study [11]. Despite a decrease in activity, all encapsulated enzymes are assumed to be active. Additionally, the substrate and product are assumed to freely enter and exit the VLP through the fixed pores. This is assumed because the pore sizes of the Qβ VLP measure up to 1.5 nm in diameter [65]. The substrate 4-nitrophenyl octanoate is significantly smaller based on bond lengths and angles.

3.5. Enzyme Stability

Overall, this work verifies the stabilizing effects of VLPs for enzymes such as CalB and the ability of open CFPS systems to directly tune and optimize packing efficiency. Significant improvements to thermal stability were observed with the encapsulation of CalB. The thermal stability results of the free enzymes indicate the irreversible loss of

structure and activity once free CalB is denatured at temperatures above its melting point because returning to the enzyme's optimum temperature did not restore functionality. By contrast, encapsulated enzymes were immobilized at the inner surface of the VLP via the RNA aptamer. The VLP possesses a high melting temperature range of 85–100 °C [66]. It is postulated that the VLP protected the enzymes by preventing complete denaturation at elevated temperatures due to the crowded environment inside the VLP. We hypothesize that in more crowded conditions the thermal stability will increase. This is due to fewer degrees of freedom to unfold in the crowded state. This is influenced by the activity–stability trade-off exhibited by many enzymes where increased stability often leads to decreased activity [67]. Given that, at increased packing densities, the activity decreased, we expect that the stability will increase. This work additionally verifies that the Qβ VLP prevented macromolecules like proteinase K from entering and degrading the enzyme. Although there was a moderate decrease in activity upon encapsulation, the thermal stability and protease resistance gained through VLP encapsulation is substantial.

4. Materials and Methods

4.1. Extract Preparation

E. coli extract was prepared as previously reported using BL21 Star™ (DE3) *E. coli* strain purchased from Invitrogen (Carlsbad, CA, USA) [68]. Briefly, the cells are lysed using a high-pressure homogenizer and then pelleted via centrifugation where the supernatant is used as the cell extract. The preparation of the cell extract for *Candida antarctica* lipase B (CalB) production was identical to the preparation for BL21 Star™ (DE3) The *E. coli* strain, except the *E. coli* strain harboring pOFX-GroEL/ES plasmid, was a gift from Dr. Dong-Myung Kim (Chungnam National University, Daejeon, Republic of Korea), and spectinomycin (100 μg/mL) was added to each culture media.

4.2. Cell-Free Protein Synthesis

The CFPS reaction of bacteriophage Qβ coat protein was carried out in a 2.0 mL size eppendorf tube at 37 °C for 3 h. Each reaction contained 25% reaction volume of the cell extract, 1.2 nM plasmid, 12 to 15 mM magnesium glutamate, 1 mM 1,4-Diaminobutane, 1.5 mM Spermidine, 33.33 mM phosphoenolpyruvate (PEP), 10 mM ammonium glutamate, 175 mM potassium glutamate, 2.7 mM potassium oxalate, 0.33 mM nicotinamide adenine dinucleotide (NAD), 0.27 mM coenzyme A (CoA), 1.2 mM ATP, 0.86 mM CTP, 0.86 mM GTP, 0.86 mM UTP, 0.17 mM folinic acid, and 2 mM of all 20 amino acids except glutamic acid. Two different plasmids were used for the coat protein: one with the histidine tag and one without. The molar ratio of non-tagged-to-tagged plasmid was 3:1.

CFPS conditions to produce of Rev-CalB were identical to CP expression, except the (1) cell extract used to express Rev-CalB contained overexpressed GroEL and GroES chaperones to aid in protein folding, (2) a 5 mM glutathione buffer (GSSG:GSH = 4:1) was added, and (3) the reaction occurred at 30 °C for 5 h.

4.3. Measuring Protein Concentration

The protein concentration was determined as previously described [69]. Briefly, C^{14}-leucine was added as a small percentage (3 μM) of the 2 mM of leucine added to the CFPS reaction and thus incorporated into synthesized protein. To determine synthesized protein concentrations, the protein was precipitated onto filter paper by washing with 5% (v/v) trichloroacetic acid (TCA) 3 times at 15 min intervals. The level of radioactivity was measured using a liquid scintillation counter from which the percentage of leucine incorporated could be determined and used to determine the total amount of protein synthesized. For

soluble protein measurements, the samples were centrifuged at 21,000 RPM for 15 min at 4 °C prior to TCA precipitation.

4.4. Bacteriophage Qβ Coat Protein Purification

The cell-free reaction that produced the Qβ coat protein was inserted into a dialysis tubing bag (Spectra/Por, Rancho Dominguez, CA, USA) with a molecular weight cut off of 6–8 kDa. The sample was immediately dialyzed against 300 mL NET buffer (150 mM NaCl and 20 mM Tris-HCl, pH 7.8). The dialyzed samples were loaded directly onto the HisPur™ Ni-NTA spin column (Thermo Scientific, Rockford, IL, USA) that was pre-equilibrated with NET buffer containing 10 mM imidazole. The column was equilibrated with sample proteins for 30 min at 4 °C and then the column was washed with a NET buffer containing 10 mM imidazole (1.2 mL). The VLPs were eluted with a NET buffer containing 500 mM imidazole (300 uL). The eluted samples were concentrated during dialysis in 500 mL NET buffer containing 40% glycerol. The purified yields were calculated with scintillation counting, using methods previously described as well as based off the densitometry analysis of the purified gels.

4.5. RNA Aptamer Transcription

The RNA aptamer was a transcription product from a DNA template. The DNA template was based on the coat protein DNA sequence. An arginine-rich peptide (Rev) tag binding sequence was fused to the 5′-end and a hairpin loop sequence that natively binds to the inner surface of the VLP was fused to the 3′-end of the coat protein DNA during the polymerase chain reaction. Both forward and reverse primers contained T7 promoter and terminator sequences, respectively, for transcription by T7 RNA polymerase. The transcribed RNA aptamer was similar to what is used for in vivo enzyme encapsulation [39]. The RNA aptamer was added to the CFPS reaction of coat protein along with Rev-CalB.

4.6. Lipase Activity

All the experiments were run in triplicate, and all the kinetic data were analyzed with respect to enzyme concentration. The activity and kinetics of free Rev-CalB (8.2 nM) and encapsulated Rev-CalB (2.13 nM) were analyzed with the substrate 4-nitrophenyl octanoate (Sigma Aldrich, Milwaukee, WI, USA), using Synergy™ Mx (BioTek, Winooski, VT, USA). The enzyme kinetics were determined using varying concentrations of the substrate (10, 42.8, 85.7, 171.4, 300, 400, and 600 µM) which were prepared in a substrate buffer (0.4 M DMSN. 0.2% triton x-100. 1× PBS) by serial dilutions. An amount of 1 µL of each varying substrate concentration was added to 70 µL of lipase reaction solution (0.4 M DMSN. 0.2% triton x-100. 1× PBS, pH 7.0) at 37 °C and read immediately. The absorbance was read at a 410 nm wavelength for hydrolyzed substrate 4-Nitrophenol. The measurements were repeated at 20 sec intervals for 20 min with 30 sec of shaking before the measurements were taken. Enzyme activity is defined as the rate of substrate hydrolysis with units of nM/s, which was determined at each substrate concentration using a molar extinction coefficient of 17,800 $M^{-1}cm^{-1}$ at 410 nm. The Michaelis–Menten analysis was performed using GraphPad Prism 10 software. The activity data were normalized to the same amount of enzyme for both free and encapsulated Rev-CalB. Specific activity is defined as the amount of hydrolyzed substrate per mg of CalB enzyme in a minute. This is calculated based off the V_{max} value and the amount of enzyme added for each condition.

4.7. Thermal Stability

Before the activity test, the enzymes were incubated at specific temperatures (37, 60, 75, and 90 °C) for 20 min using a thermocycler (Biorad, Hercules, CA, USA), followed by incubation at 37 °C for 1 h. An amount of 1 µL of 12 mM substrate was added to each

70 µL lipase reaction solution. The substrate working concentration was 171.4 µM. The concentrations of both free and encapsulated lipases were 8.2 µM and 2.13 µM, respectively.

4.8. Protease Stability

Proteinase K was purchased from Thermofisher Scientific (Fairlawn, NJ, USA) in order to perform the enzyme stability test. A 100 µL stock solution was prepared in NET buffer containing 40% glycerol with 20 mg of Proteinase K powder (0.2 mg/µL). The stock protease solution was diluted to a concentration of 0.002 mg/µL by serial dilution using the lipase reaction solution. Both the free and encapsulated Rev-CalB were pre-incubated at 37 °C for an hour before adding the protease. They were then incubated with Proteinase K for 0, 30, 60, 180, and 300 min at 37 °C. After the protease incubation, the activity of the enzymes was measured with the substrate, as described previously.

4.9. Protein Separation and Autoradiography to Determine the Ratio of VLP and Rev-CalB

The proteins produced from the CFPS reactions were loaded onto SDS-PAGE with 10% bis-tris gels (Invitrogen, Carlsbad, CA, USA) for protein separation and stained with SimplyBlue SafeStain (Invitrogen). The PAGE gels were dried on a Whatman 3MM chromatography paper at 80 °C for 2 h using a vacuum pump. The dried gels were exposed to Kodak BioMax MR autoradiography film (Rochester, NY, USA) for 10 days. Densitometry measurements were performed using ImageJ software v1.50 [65]. The VLP and Rev-CalB have different molecular weights (14 kDa—monomer and 37 kDa, respectively) and were found at different locations in the SDS-PAGE gel. Both the VLP and enzymes were incorporated with C^{14}-leucine, and relative band intensities were used to measure the number of enzymes enclosed per VLP. Figure 2a was created by cropping the ladder portion of the figure (left) from the original SDS-PAGE gel image. The autoradiogram portion of the image (right) was cropped from the original autoradiogram image and uniformly brightened before aligning it with the ladder.

4.10. TEM Imaging

The protein samples were dried on the formvar-coated copper grid (Electron Microscopy Sciences, Hatfield, PA, USA) for 1 min. The dried samples were soaked with 2% phosphotungstic acid for 1 min and then dried. The images were digitally captured by Tecnai T-12 and Tecnai 23 T-20 TEM (FEI, Hillsboro, OR, USA; Gatan, Pleasanton, CA, USA) at a 120 kV and 200 kV acceleration voltage, respectively. ImageJ software was used to estimate the diameter of the VLPs [65]. Figure 2b,c are original images with arrows added to point out VLP locations.

5. Conclusions

Here, we developed a simple in vitro three-step process using CFPS that allows us to produce, encapsulate, and purify biocatalysts inside a VLP. VLP encapsulation enables significantly improved stability against protease activity and incubation at temperatures above the known enzyme melting temperature. The designed method does not require guest enzyme purification and the VLP is engineered with a His-tag for facile rapid purification. The desired amount of guest enzymes for encapsulation determines the encapsulation efficiency and can be readily optimized with the CFPS system demonstrated. In this study, the industrially relevant enzyme CalB's activity was largely intact upon encapsulation and the enzyme is stabilized against high temperatures and protease degradation. This process has the potential to be applied to a wide variety of biocatalyst applications allowing for the rapid optimization and production of stable enzymes through VLP encapsulation.

Supplementary Materials: The following supporting information can be downloaded at https://www.mdpi.com/article/10.3390/synbio3010005/s1: Figure S1: Size Exclusion Purification of Qβ VLP Assembled from CFPS reaction with sfGFP; Figure S2: The original images for Figure 2a in the main text; Figure S3: Purification gels and autoradiograms for the encapsulated enzymes.

Author Contributions: Conceptualization, S.O.Y. and B.C.B.; methodology, S.O.Y. and B.C.B.; software, S.O.Y. and J.P.T.; validation, S.O.Y.; formal analysis, S.O.Y., J.P.T., G.H.N., K.M.W. and B.C.B.; investigation, S.O.Y.; resources, B.C.B.; data curation, S.O.Y.; writing—original draft preparation, S.O.Y., J.P.T., G.H.N., K.M.W. and B.C.B.; writing—review and editing, S.O.Y., J.P.T., G.H.N., K.M.W. and B.C.B.; visualization, S.O.Y., J.P.T. and B.C.B.; supervision, B.C.B.; project administration, S.O.Y. and B.C.B.; and funding acquisition, B.C.B. All authors have read and agreed to the published version of the manuscript.

Funding: This research was funded by the Simmons Center for Cancer Research at Brigham Young University.

Institutional Review Board Statement: Not applicable.

Informed Consent Statement: Not applicable.

Data Availability Statement: The data presented in this study are available within the article's supplementary information.

Acknowledgments: The authors gratefully acknowledge Dallin Chipman for assistance in gathering citations.

Conflicts of Interest: The authors declare no conflicts of interest.

References

1. Lu, L.; Guo, L.; Wang, K.; Liu, Y.; Xiao, M. β-Galactosidases: A great tool for synthesizing galactose-containing carbohydrates. *Biotechnol. Adv.* **2020**, *39*, 107465. [CrossRef] [PubMed]
2. Dutta, S.; Adhikary, S.; Bhattacharya, S.; Roy, D.; Chatterjee, S.; Chakraborty, A.; Banerjee, D.; Ganguly, A.; Nanda, S.; Rajak, P. Contamination of textile dyes in aquatic environment: Adverse impacts on aquatic ecosystem and human health, and its management using bioremediation. *J. Environ. Manag.* **2024**, *353*, 120103. [CrossRef] [PubMed]
3. Sonawane, P.D.; Gharat, S.A.; Jozwiak, A.; Barbole, R.; Heinicke, S.; Almekias-Siegl, E.; Meir, S.; Rogachev, I.; Connor, S.E.O.; Giri, A.P. A BAHD-type acyltransferase concludes the biosynthetic pathway of non-bitter glycoalkaloids in ripe tomato fruit. *Nat. Commun.* **2023**, *14*, 4540. [CrossRef] [PubMed]
4. Gonçalves, M.C.P.; Amaral, J.C.; Fernandez-Lafuente, R.; Junior, R.d.S.; Tardioli, P.W. Lipozyme 435-mediated synthesis of xylose oleate in methyl ethyl ketone. *Molecules* **2021**, *26*, 3317. [CrossRef] [PubMed]
5. Li, B.; Tian, J.; Zhang, F.; Wu, C.; Li, Z.; Wang, D.; Zhuang, J.; Chen, S.; Song, W.; Tang, Y. Self-assembled aldehyde dehydrogenase-activatable nano-prodrug for cancer stem cell-enriched tumor detection and treatment. *Nat. Commun.* **2024**, *15*, 9417. [CrossRef]
6. Liu, Y.; Jiang, J.-J.; Du, S.-Y.; Mu, L.-S.; Fan, J.-J.; Hu, J.-C.; Ye, Y.; Ding, M.; Zhou, W.-Y.; Yu, Q.-H. Artemisinins ameliorate polycystic ovarian syndrome by mediating LONP1-CYP11A1 interaction. *Science* **2024**, *384*, eadk5382. [CrossRef]
7. Das, S.; Zhao, L.; Elofson, K.; Finn, M.G. Enzyme Stabilization by Virus-Like Particles. *Biochemistry* **2020**, *59*, 2870–2881. [CrossRef]
8. Kambiré, M.S.; Gnanwa, J.M.; Boa, D.; Kouadio, E.J.P.; Kouamé, L.P. Modeling of enzymatic activity of free β-glucosidase from palm weevil, Rhynchophorus palmarum Linn. (Coleoptera: Curculionidae) larvae: Effects of pH and temperature. *Biophys. Chem.* **2021**, *276*, 106611. [CrossRef]
9. Caglayan, C.; Taslimi, P.; Türk, C.; Gulcin, İ.; Kandemir, F.M.; Demir, Y.; Beydemir, Ş. Inhibition effects of some pesticides and heavy metals on carbonic anhydrase enzyme activity purified from horse mackerel (*Trachurus trachurus*) gill tissues. *Environ. Sci. Pollut. Res.* **2020**, *27*, 10607–10616. [CrossRef]
10. Minten, I.J.; Claessen, V.I.; Blank, K.; Rowan, A.E.; Nolte, R.J.M.; Cornelissen, J.J.L.M. Catalytic capsids: The art of confinement. *Chem. Sci.* **2011**, *2*, 358–362. [CrossRef]
11. Patterson, D.P.; Prevelige, P.E.; Douglas, T. Nanoreactors by programmed enzyme encapsulation inside the capsid of the bacteriophage P22. *ACS Nano* **2012**, *6*, 5000–5009. [CrossRef] [PubMed]
12. Worsdorfer, B.; Woycechowsky, K.J.; Hilvert, D. Directed evolution of a protein container. *Science* **2011**, *331*, 589–592. [CrossRef] [PubMed]
13. Kermasha, S.; Gill, J.K. Chapter Six—Immobilization of enzymes and their use in biotechnological applications. In *Enzymes*; Kermasha, S., Eskin, M.N.A., Eds.; Academic Press: San Diego, CA, USA, 2021; pp. 133–170.

14. Yamaguchi, A.; Nakayama, H.; Morita, Y.; Sakamoto, H.; Kitamura, T.; Hashimoto, M.; Suye, S.-i. Enhanced and Prolonged Activity of Enzymes Adsorbed on TEMPO-Oxidized Cellulose Nanofibers. *ACS Omega* **2020**, *5*, 18826–18830. [CrossRef] [PubMed]
15. Lu, X.; Zheng, X.; Li, X.; Zhao, J. Adsorption and mechanism of cellulase enzymes onto lignin isolated from corn stover pretreated with liquid hot water. *Biotechnol. Biofuels* **2016**, *9*, 118. [CrossRef]
16. Smith, M.T.; Wu, J.C.; Varner, C.T.; Bundy, B.C. Enhanced protein stability through minimally invasive, direct, covalent, and site-specific immobilization. *Biotechnol. Prog.* **2013**, *29*, 247–254. [CrossRef]
17. Rodrigues, R.C.; Berenguer-Murcia, Á.; Carballares, D.; Morellon-Sterling, R.; Fernandez-Lafuente, R. Stabilization of enzymes via immobilization: Multipoint covalent attachment and other stabilization strategies. *Biotechnol. Adv.* **2021**, *52*, 107821. [CrossRef]
18. Wu, J.C.; Hutchings, C.H.; Lindsay, M.J.; Werner, C.J.; Bundy, B.C. Enhanced enzyme stability through site-directed covalent immobilization. *J. Biotechnol.* **2015**, *193*, 83–90. [CrossRef]
19. Imam, H.T.; Marr, P.C.; Marr, A.C. Enzyme entrapment, biocatalyst immobilization without covalent attachment. *Green Chem.* **2021**, *23*, 4980–5005. [CrossRef]
20. Sharma, M.; Sharma, V.; Majumdar, D.K. Entrapment of alpha-Amylase in Agar Beads for Biocatalysis of Macromolecular Substrate. *Int. Sch. Res. Not.* **2014**, *2014*, 936129. [CrossRef]
21. Zhang, H.; Feng, M.; Fang, Y.; Wu, Y.; Liu, Y.; Zhao, Y.; Xu, J. Recent advancements in encapsulation of chitosan-based enzymes and their applications in food industry. *Crit. Rev. Food Sci. Nutr.* **2023**, *63*, 11044–11062. [CrossRef]
22. Bhushan, B.; Pal, A.; Jain, V. Improved Enzyme Catalytic Characteristics upon Glutaraldehyde Cross-Linking of Alginate Entrapped Xylanase Isolated from Aspergillus flavus MTCC 9390. *Enzym. Res.* **2015**, *2015*, 210784. [CrossRef] [PubMed]
23. Charoenwongpaiboon, T.; Wangpaiboon, K.; Field, R.A.; Prousoontorn, M.; Pichyangkura, R. Cross-linked enzyme aggregates (combi-CLEAs) derived from levansucrase and variant inulosucrase are highly efficient catalysts for the synthesis of levan-type fructooligosaccharides. *Mol. Catal.* **2023**, *535*, 112827. [CrossRef]
24. González-Davis, O.; Villagrana-Escareño, M.V.; Trujillo, M.A.; Gama, P.; Chauhan, K.; Vazquez-Duhalt, R. Virus-like nanoparticles as enzyme carriers for Enzyme Replacement Therapy (ERT). *Virology* **2023**, *580*, 73–87. [CrossRef] [PubMed]
25. Chauhan, K.; Olivares-Medina, C.N.; Villagrana-Escareño, M.V.; Juárez-Moreno, K.; Cadena-Nava, R.D.; Rodríguez-Hernández, A.G.; Vazquez-Duhalt, R. Targeted Enzymatic VLP-Nanoreactors with β-Glucocerebrosidase Activity as Potential Enzyme Replacement Therapy for Gaucher's Disease. *ChemMedChem* **2022**, *17*, e202200384. [CrossRef]
26. McNeale, D.; Dashti, N.; Cheah, L.C.; Sainsbury, F. Protein cargo encapsulation by virus-like particles: Strategies and applications. *WIREs Nanomed. Nanobiotechnol.* **2023**, *15*, e1869. [CrossRef]
27. Jordan, P.C.; Patterson, D.P.; Saboda, K.N.; Edwards, E.J.; Miettinen, H.M.; Basu, G.; Thielges, M.C.; Douglas, T. Self-assembling biomolecular catalysts for hydrogen production. *Nat. Chem.* **2016**, *8*, 179–185. [CrossRef]
28. Rampoldi, A.; Crooke, S.N.; Preininger, M.K.; Jha, R.; Maxwell, J.; Ding, L.; Spearman, P.; Finn, M.G.; Xu, C. Targeted Elimination of Tumorigenic Human Pluripotent Stem Cells Using Suicide-Inducing Virus-like Particles. *ACS Chem. Biol.* **2018**, *13*, 2329–2338. [CrossRef]
29. Su, Y.; Liu, B.; Huang, Z.; Teng, Z.; Yang, L.; Zhu, J.; Huo, S.; Liu, A. Virus-like particles nanoreactors: From catalysis towards bio-applications. *J. Mater. Chem. B* **2023**, *11*, 9084–9098. [CrossRef]
30. Sharma, J.; Uchida, M.; Miettinen, H.M.; Douglas, T. Modular interior loading and exterior decoration of a virus-like particle. *Nanoscale* **2017**, *9*, 10420–10430. [CrossRef]
31. Fiedler, J.D.; Fishman, M.R.; Brown, S.D.; Lau, J.; Finn, M. Multifunctional enzyme packaging and catalysis in the Qβ protein nanoparticle. *Biomacromolecules* **2018**, *19*, 3945–3957. [CrossRef]
32. Garenne, D.; Bowden, S.; Noireaux, V. Cell-free expression and synthesis of viruses and bacteriophages: Applications to medicine and nanotechnology. *Curr. Opin. Syst. Biol.* **2021**, *28*, 100373. [CrossRef]
33. Schwarz, B.; Uchida, M.; Douglas, T. Biomedical and catalytic opportunities of virus-like particles in nanotechnology. *Adv. Virus Res.* **2017**, *97*, 1–60. [PubMed]
34. Mejía-Méndez, J.L.; Vazquez-Duhalt, R.; Hernández, L.R.; Sánchez-Arreola, E.; Bach, H. Virus-like particles: Fundamentals and biomedical applications. *Int. J. Mol. Sci.* **2022**, *23*, 8579. [CrossRef] [PubMed]
35. Fiedler, J.D.; Higginson, C.; Hovlid, M.L.; Kislukhin, A.A.; Castillejos, A.; Manzenrieder, F.; Campbell, M.G.; Voss, N.R.; Potter, C.S.; Carragher, B.; et al. Engineered mutations change the structure and stability of a virus-like particle. *Biomacromolecules* **2012**, *13*, 2339–2348. [CrossRef]
36. Smith, M.T.; Varner, C.T.; Bush, D.B.; Bundy, B.C. The incorporation of the A2 protein to produce novel Qbeta virus-like particles using cell-free protein synthesis. *Biotechnol. Prog.* **2012**, *28*, 549–555. [CrossRef]
37. Weber, H. The binding site for coat protein on bacteriophage Qbeta RNA. *Biochim. et Biophys. Acta* **1976**, *418*, 175–183. [CrossRef]
38. Witherell, G.W.; Uhlenbeck, O.C. Specific RNA binding by Q beta coat protein. *Biochemistry* **1989**, *28*, 71–76. [CrossRef]
39. Fiedler, J.D.; Brown, S.D.; Lau, J.L.; Finn, M.G. RNA-directed packaging of enzymes within virus-like particles. *Angew. Chem. (Int. Ed. Engl.)* **2010**, *49*, 9648–9651. [CrossRef]

40. Golmohammadi, R.; Fridborg, K.; Bundule, M.; Valegard, K.; Liljas, L. The crystal structure of bacteriophage Q beta at 3.5 A resolution. *Structure* **1996**, *4*, 543–554. [CrossRef]
41. Boles, K.S.; Kannan, K.; Gill, J.; Felderman, M.; Gouvis, H.; Hubby, B.; Kamrud, K.I.; Venter, J.C.; Gibson, D.G. Digital-to-biological converter for on-demand production of biologics. *Nat. Biotechnol.* **2017**, *35*, 672–675. [CrossRef]
42. Smith, M.T.; Wilding, K.M.; Hunt, J.M.; Bennett, A.M.; Bundy, B.C. The emerging age of cell-free synthetic biology. *FEBS Lett.* **2014**, *588*, 2755–2761. [CrossRef] [PubMed]
43. Salehi, A.S.; Smith, M.T.; Bennett, A.M.; Williams, J.B.; Pitt, W.G.; Bundy, B.C. Cell-free protein synthesis of a cytotoxic cancer therapeutic: Onconase production and a just-add-water cell-free system. *Biotechnol. J.* **2015**, *11*, 274–281. [CrossRef] [PubMed]
44. Shrestha, P.; Smith, M.T.; Bundy, B.C. Cell-free unnatural amino acid incorporation with alternative energy systems and linear expression templates. *New Biotechnol.* **2014**, *31*, 28–34. [CrossRef] [PubMed]
45. Salehi, A.S.; Earl, C.C.; Muhlestein, C.; Bundy, B.C. *Escherichia coli*-based cell-free extract development for protein-based cancer therapeutic production. *Int. J. Dev. Biol.* **2016**, *60*, 237–243. [CrossRef] [PubMed]
46. Blank, K.; Morfill, J.; Gumpp, H.; Gaub, H.E. Functional expression of *Candida antarctica* lipase B in *Eschericha coli*. *J. Biotechnol.* **2006**, *125*, 474–483. [CrossRef]
47. Park, C.G.; Kim, T.W.; Oh, I.S.; Song, J.K.; Kim, D.M. Expression of functional *Candida antarctica* lipase B in a cell-free protein synthesis system derived from *Escherichia coli*. *Biotechnol. Prog.* **2009**, *25*, 589–593. [CrossRef]
48. Anderson, E.M.; Larsson, K.M.; Kirk, O. One biocatalyst-many applications: The use of *Candida antarctica* B-lipase in organic synthesis. *Biocatal. Biotransform.* **1998**, *16*, 181–204. [CrossRef]
49. Van Tassel, L.; Moilanen, A.; Ruddock, L.W. Efficient production of wild-type lipase B from *Candida antarctica* in the cytoplasm of *Escherichia coli*. *Protein Expr. Purif.* **2020**, *165*, 105498. [CrossRef]
50. Lu, C.; Peng, X.; Lu, D.; Liu, Z. Global and Kinetic Profiles of Substrate Diffusion in *Candida antarctica* Lipase B: Molecular Dynamics with the Markov-State Model. *ACS Omega* **2020**, *5*, 9806–9812. [CrossRef]
51. Uppenberg, J.; Hansen, M.T.; Patkar, S.; Jones, T.A. The sequence, crystal structure determination and refinement of two crystal forms of lipase B from *Candida antarctica*. *Structure* **1994**, *2*, 293–308. [CrossRef]
52. Stauch, B.; Fisher, S.J.; Cianci, M. Open and closed states of *Candida antarctica* lipase B: Protonation and the mechanism of interfacial activation. *J. Lipid Res.* **2015**, *56*, 2348–2358. [CrossRef] [PubMed]
53. Wilding, K.M.; Hunt, J.P.; Wilkerson, J.W.; Funk, P.J.; Swensen, R.L.; Carver, W.C.; Christian, M.L.; Bundy, B.C. Endotoxin-free *E. coli*-based cell-free protein synthesis: Pre-expression endotoxin removal approaches for on-demand cancer therapeutic production. *Biotechnol. J.* **2018**, *14*, 1800271. [CrossRef] [PubMed]
54. Burdette, R.A.; Quinn, D.M. Interfacial reaction dynamics and acyl-enzyme mechanism for lipoprotein lipase-catalyzed hydrolysis of lipid p-nitrophenyl esters. *J. Biol. Chem.* **1986**, *261*, 12016–12021. [CrossRef] [PubMed]
55. Ulker, C.; Gokalp, N.; Guvenilir, Y. Immobilization of *Candida antarctica* lipase B (CALB) on surface-modified rice busk ashes (RHA) via physical adsorption and cross-linking methods. *Biocatal. Biotransform.* **2016**, *34*, 172–180. [CrossRef]
56. Zhang, N.; Suen, W.C.; Windsor, W.; Xiao, L.; Madison, V.; Zaks, A. Improving tolerance of *Candida antarctica* lipase B towards irreversible thermal inactivation through directed evolution. *Protein Eng.* **2003**, *16*, 599–605. [CrossRef]
57. Kim, S.K.; Park, Y.C.; Lee, H.H.; Jeon, S.T.; Min, W.K.; Seo, J.H. Simple amino acid tags improve both expression and secretion of *Candida antarctica* lipase B in recombinant *Escherichia coli*. *Biotechnol. Bioeng.* **2015**, *112*, 346–355. [CrossRef]
58. Xu, C.; Suo, H.; Xue, Y.; Qin, J.; Chen, H.; Hu, Y. Experimental and theoretical evidence of enhanced catalytic performance of lipase B from *Candida antarctica* acquired by the chemical modification with amino acid ionic liquids. *Mol. Catal.* **2021**, *501*, 111355. [CrossRef]
59. Xue, Y.; Zhang, X.-G.; Lu, Z.-P.; Xu, C.; Xu, H.-J.; Hu, Y. Enhancing the Catalytic Performance of *Candida antarctica* Lipase B by Chemical Modification with Alkylated Betaine Ionic Liquids. *Front. Bioeng. Biotechnol.* **2022**, *10*, 850890. [CrossRef]
60. Xiao, D.; Li, X.; Zhang, Y.; Wang, F. Efficient Expression of *Candida antarctica* Lipase B in Pichia pastoris and Its Application in Biodiesel Production. *Appl. Biochem. Biotechnol.* **2023**, *195*, 5933–5949. [CrossRef]
61. Cassimjee, K.E.; Hendil-Forssell, P.; Volkov, A.; Krog, A.; Malmo, J.; Aune, T.E.V.; Knecht, W.; Miskelly, I.R.; Moody, T.S.; Svedendahl Humble, M. Streamlined Preparation of Immobilized *Candida antarctica* Lipase B. *ACS Omega* **2017**, *2*, 8674–8677. [CrossRef]
62. Ujiie, A.; Nakano, H.; Iwasaki, Y. Extracellular production of Pseudozyma (Candida) antarctica lipase B with genuine primary sequence in recombinant *Escherichia coli*. *J. Biosci. Bioeng.* **2016**, *121*, 303–309. [CrossRef] [PubMed]
63. Xie, Y.; An, J.; Yang, G.; Wu, G.; Zhang, Y.; Cui, L.; Feng, Y. Enhanced enzyme kinetic stability by increasing rigidity within the active site. *J. Biol. Chem.* **2014**, *289*, 7994–8006. [CrossRef] [PubMed]
64. Zisis, T.; Freddolino, P.L.; Turunen, P.; van Teeseling, M.C.; Rowan, A.E.; Blank, K.G. Interfacial activation of *Candida antarctica* lipase B: Combined evidence from experiment and simulation. *Biochemistry* **2015**, *54*, 5969–5979. [CrossRef] [PubMed]

65. Gorzelnik, K.V.; Cui, Z.; Reed, C.A.; Jakana, J.; Young, R.; Zhang, J. Asymmetric cryo-EM structure of the canonical Allolevivirus Qβ reveals a single maturation protein and the genomic ssRNA in situ. *Proc. Natl. Acad. Sci. USA* **2016**, *113*, 11519–11524. [CrossRef]
66. Ashcroft, A.E.; Lago, H.; Macedo, J.M.; Horn, W.T.; Stonehouse, N.J.; Stockley, P.G. Engineering thermal stability in RNA phage capsids via disulphide bonds. *J. Nanosci. Nanotechnol.* **2005**, *5*, 2034–2041. [CrossRef]
67. Hou, Q.; Rooman, M.; Pucci, F. Enzyme stability-activity trade-off: New insights from protein stability weaknesses and evolutionary conservation. *J. Chem. Theory Comput.* **2023**, *19*, 3664–3671. [CrossRef]
68. Bundy, B.C.; Swartz, J.R. Efficient disulfide bond formation in virus-like particles. *J. Biotechnol.* **2011**, *154*, 230–239. [CrossRef]
69. Jewett, M.C.; Swartz, J.R. Rapid expression and purification of 100 nmol quantities of active protein using cell-free protein synthesis. *Biotechnol. Prog.* **2004**, *20*, 102–109. [CrossRef]